Biosensors and Bioelectronics 74 (2015) 637–643

Contents lists available at ScienceDirect

Biosensors and Bioelectronics

journal homepage: www.elsevier.com/locate/bios

Development of L-lactate dehydrogenase biosensor based on porous silicon resonant microcavities as fluorescence enhancers

S.N. Aisyiyah Jenie, Beatriz Prieto-Simon, Nicolas H. Voelcker*

ARC Centre of Excellence in Convergent Bio-Nano Science and Technology, Mawson Institute, University of South Australia, Mawson Lakes, SA 5095, Australia

ARTICLE INFO

Article history:
Received 22 May 2015
Received in revised form
10 July 2015
Accepted 11 July 2015
Available online 13 July 2015

Keywords:
Lactate dehydrogenase
Porous silicon
Microcavity
Fluorescence enhancement
Biosensor

ABSTRACT

The up-regulation of L-lactate dehydrogenase (LDH), an intracellular enzyme present in most of all body tissues, is indicative of several pathological conditions and cellular death. Herein, we demonstrate LDH detection using porous silicon (pSi) microcavities as a luminescence-enhancing optical biosensing platform. Non-fluorescent resazurin was covalently attached onto the pSi surface *via* thermal hydrocarbonisation, thermal hydrosylilation and acylation. Each surface modification step was confirmed by means of FTIR and the optical shifts of the resonance wavelength of the microcavity. Thermal hydrocarbonisation also afforded excellent surface stability, ensuring that the resazurin was not reduced on the pSi surface. Using a pSi microcavity biosensor, the fluorescence signal upon detection of LDH was amplified by 10 and 5-fold compared to that of a single layer and a detuned microcavity, respectively, giving a limit of detection of 0.08 U/ml. The biosensor showed a linear response between 0.16 and 6.5 U/ml, covering the concentration range of LDH in normal as well as damaged tissues. The biosensor was selective for LDH and did not produce a signal upon incubation with another NAD-dependant enzyme L-glutamic dehydrogenase. The use of the pSi microcavity as a sensing platform reduced reagent usage by 30% and analysis time threefold compared to the standard LDH assay in solution.

1. Introduction

Enzymatic sensors have received a great deal of attention over the past decades. These biosensors possess high selectivity: the enzyme reacts with its enzymatic substrate under specific reaction conditions, such as pH, temperature and ionic strength (Bisswanger, 2014). Besides being known for high selectivity and specificity, enzyme-based sensors are also sensitive, rapid and can be used for real-time monitoring of target analytes of interest in clinical analysis (Ispas et al., 2012). One of the most common physiological markers in disease diagnosis is the enzyme L-lactate dehydrogenase (LDH) (Chen et al., 2006; Drent et al., 1996; Kato et al., 2006; Moran and Schnellmann, 1996). LDH is an intracellular enzyme present in most of all body tissues (Drent et al., 1996). The enzyme is built upon four peptide chains either forming from the heart or from the muscle. The main biochemical property of LDH is as a hydrogen transfer enzyme, catalysing the reversible reaction of L-lactate to pyruvate through the reduction of the coenzyme nicotinamide-adenine dinucleotide (NAD^+). NAD^+ acts as a hydrogen acceptor forming the reduced form, NADH. LDH is released from damaged tissues, hence the increase of LDH levels in the blood is indicative of a pathological condition, making it one of the most important markers of injury or disease. The up-regulation of this enzyme has been reported to serve as an aid for early detection of cell death levels (Moran and Schnellmann, 1996) and is correlated with conditions such as pulmonary cancer (Hou et al., 2009), leukaemia (Kastritis et al., 2010), melanoma (Ho et al., 2012) and chronic wounds (James et al., 2000). Due to its significance in the early stage of disease diagnosis, sensitive biosensors capable of monitoring LDH activity have recently grown in importance (Kastritis et al., 2010; Kato et al., 2006).

Currently LDH assay kits for cytotoxicity and cell damage evaluations are commercially available. As described in the protocols, these assay kits rely on the monitoring of the absorbance peak of a tetrazolium dye (Decker and Lohmann-Matthes, 1988). When compared to the absorbance-based detection, fluorescence-based detection has been reported to be more sensitive since the fluorescence intensity is proportional to the excitation intensity, hence the system is capable to detect weak signals (Bosch et al., 2007). The release of LDH *via* the distinctly different fluorescence properties of NADH and NAD^+ has been reported (Moran and Schnellmann, 1996; Zhu et al., 2010; Zhuang et al., 2007). NADH itself is a natural fluorophore coenzyme owing to its reduced nicotinamide ring, with an excitation wavelength of 340 nm, a maximum emission at 460 nm and a fluorescence lifetime of 0.4 ns

* Correspondence to:
GPO Box 2471, Adelaide, SA 5001, Australia. Fax: +61 8 8302 5613.
E-mail address: nico.voelcker@unisa.edu.au (N.H. Voelcker).

http://dx.doi.org/10.1016/j.bios.2015.07.025
0956-5663/

in aqueous buffer. Therefore, when LDH catalyses pyruvate into L-lactate, NADH is oxidised into NAD^+ and consequently the fluorescence is attenuated (Drent et al., 1996; Wang et al., 2008). However, the drawback of this detection system is that the low excitation wavelength at 340 nm may damage the cells when the assay is conducted *in vivo*.

Recent improvements of the fluorescence-based detection involves coupling of the above reaction with the reduction reaction of resazurin (7-hydroxy-3H-phenoxazin-3-one-10-dioxide) into resorufin (7-hydroxy-3H-phenoxazin-3-one) (Larsen, 2005). Resazurin, known as Alamar Blue (O'Brien et al., 2000), is only weakly fluorescent in its pure form. The compound consists of a phenoxazine group which contains a heterocylic N-oxide group that loses its oxygen upon reduction and forms the strongly fluorescent product, resorufin (ex/em 545 nm/583 nm). The reduction of the dye into resorufin procedes by accepting electrons from NADH and NADPH (Das et al., 2013; O'Brien et al., 2000; Candeias et al., 1998). This indirect detection is advantageous as the excitation and maximum emission wavelengths of resorufin are higher than that of NADH, thus avoiding damaging of cells and background autofluorescence. Moreover, a relatively quick response within 4–7 min after the initiation of the reaction has been reported (Larsen, 2005) as compared to the 30 min incubation time in standard LDH assays. The use of fluorescent nanoparticles, such as the ones based on quantum dots (QDs), has also been applied for LDH sensing (He et al., 2012; Ren et al., 2010; Yang et al., 2011). When LDH and its substrate, L-lactate, are present in a solution of NAD^+-modified QDs, the enzymatic reaction reduces NAD^+ into NADH followed by an increase in the luminescence intensity of the QDs. The increase of emission is a linear function of the activity of LDH.

The application of porous silicon (pSi) as a sensitive platform for enzyme monitoring has been addressed in studies (DeLouise et al., 2005; Krismastuti et al., 2013; Martin et al., 2009; Palestino et al., 2009). The excellent performance of pSi-based sensors relies on the advantageous properties of pSi (Bosch et al., 2007; Jane et al., 2009; Janshoff et al., 1998; Lin et al., 1997; Sailor and Wu, 2009; Zhao et al., 2010). Specifically, pSi with a microcavity structure offers signal amplification for fluorescence or luminescence-based detection systems. This is because the microcavity, which is a multilayer consisting of alternating porosities and a spacer layer in between, is able to enhance the emission of a fluorophore confined in the porous structure according to the Purcell effect (DeLouise and Ouyang, 2009; Koenderink, 2010; Poitras et al., 2003; Purcell, 1946; Qiao et al., 2010; Setzu et al., 2000). This particular pSi architecture has therefore been applied to fluorescence biosensor applications (Krismastuti et al., 2014; Palestino et al., 2008, 2009; Sciacca et al., 2009).

Herein, we demonstrate the detection of LDH by monitoring the emission of the reduced form of resazurin, resorufin. Two pathways of surface modification (Scheme 1) were tested on the microcavity to investigate the redox stability of immobilised resazurin on the pSi surface. The resazurin-modified pSi microcavity surface was then used as the detection platform for LDH sensing.

2. Materials and methods

2.1. Preparation of pSi microcavity (MC)

pSi samples were prepared from boron doped, [100]-oriented silicon wafers (0.00055–0.001 Ω cm specific resistivity, 475–525 μm thickness, Siltronix, France). The wafers were electrochemically etched in a 1:1 mixture of 48% (v/v) hydrofluoric acid (HF) (Scharlau, Australia) and ethanol (100%, ChemSupply, Australia) in a custom-built Teflon cell at 25 °C using a source metre (Keithley, USA) as the current source. The cathode used was a platinum mesh and aluminium foil was used to contact the silicon anode. The area of the exposed region of the silicon wafer was 1.76 cm^2. Prior to sample preparation, the parasitic layer of the samples was removed by etching the silicon wafers in a 1:1 HF/EtOH solution at 56.8 mA/cm^2 for 30 s, thorough rinsing with ethanol, drying with N_2 gas and immersing the layer in 1 M sodium hydroxide (NaOH, Merck, Australia) for 2 min. Finally, the wafer was cleaned with deionised water and ethanol consecutively before being dried under N_2 gas (Pace et al., 2013).

2.2. Modification of the pSi surface

Modification of pSi was accomplished following the steps shown in Scheme 1. In the first pathway, thermal hydrosilylation was conducted for freshly etched samples in neat undecylenic acid (Sigma-Aldrich, Australia) at 120 °C for 3 h. The functionalised surface was rinsed with pure ethanol and dried under a stream of N_2 gas. In the second pathway, freshly etched pSi samples were stabilised using thermal hydrocarbonisation under acetylene gas at 500 °C for 10 min followed by thermal hydrosilylation with neat undecylenic acid at 150 °C for 24 h. The functionalised surface was rinsed with pure ethanol and dried under a stream of N_2 gas. The samples were then immersed in neat thionyl chloride (Sigma-Aldrich, Australia) at room temperature for 10 min, followed by subsequent wash with dichloromethane and drying under a stream of N_2 gas.

pSi modification with resazurin was achieved by incubating the thionyl chloride-modified samples in a 1 mg/ml solution of resazurin (Thermo-Fisher, Australia) prepared in 4-(2-hydroxyethyl)-1-piperazineethanesulfonic acid (HEPES, Sigma-Aldrich, Australia) buffer at room temperature for 10 min and protected from light. Afterwards, the samples were rinsed with HEPES buffer and water, and dried under a stream of N_2 gas.

2.3. LDH detection

The detection of LDH (EC1.1.1.27 from chicken heart, 258 U/mg protein, ProspecBio, USA) *via* fluorescence enhancement was conducted on the pSiMC and the single layer pSi samples. Resazurin-functionalised samples were immersed in a 100 μl solution of β-NAD^+ (1 mM, Sigma-Aldrich Australia), L-lactate (35 mM, Sigma-Aldrich, Australia), PMS^+ (300 μM) and different concentrations of LDH ranging from 0.02 to 16.26 U/ml in Tris-buffer.

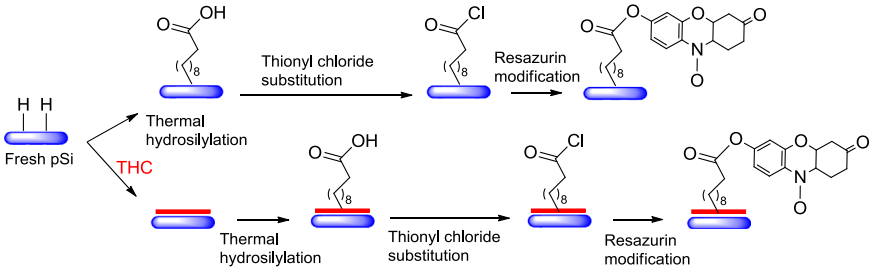

Scheme 1. Modification pathways of the pSi surface.

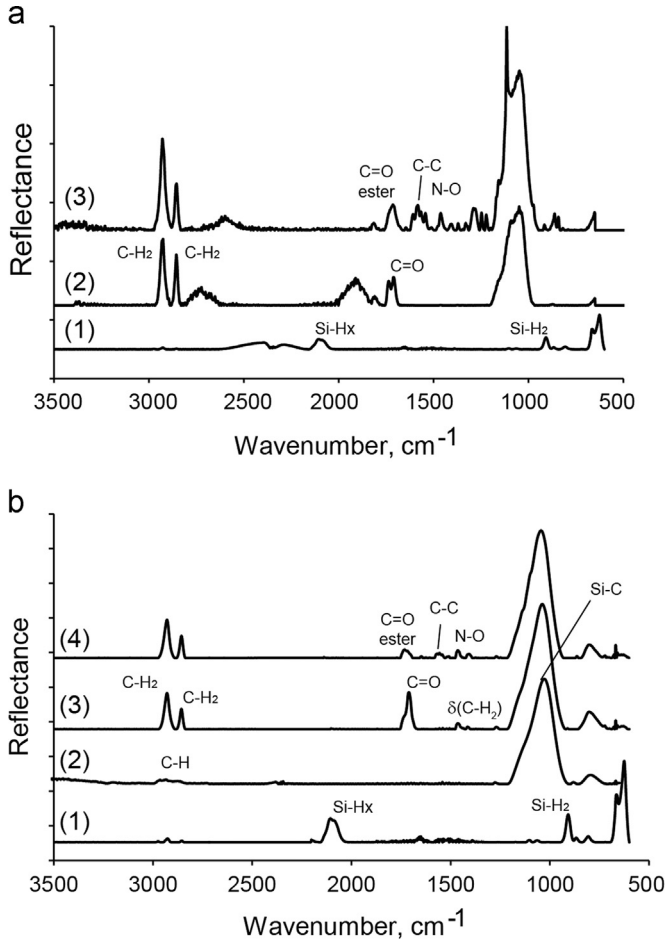

Fig. 1. Reflectance mode FT-IR spectra (baseline corrected) of the pSi samples. (a) Without THC: (1) freshly etched samples; (2) samples after thermal hydrosilylation and (3) samples after resazurin immobilisation. (b) With THC: (1) freshly etched samples; (2) samples after THC; (3) samples after thermal hydrosilylation and (4) resazurin-modified samples.

The samples were incubated at 37 °C for 10 min, rinsed with buffer, followed by DI water and gently dried under N_2 gas. Samples were placed in a quartz cuvette with a customised holder and the fluorescence intensity of the pSi samples was recorded over the range from 500 to 650 nm, with the excitation wavelength at 545 nm. Measurements were performed in triplicate.

3. Results and discussion

3.1. Characterisation of pSi surfaces

The sensing platform used in this work is based on pSi with a microcavity structure. pSiMCs feature a spacer layer with certain porosity and thickness between multilayers of high and low refractive indexes (*i.e.* porosity) or Bragg reflectors. A spacer layer with an optical thickness of $\lambda/2$ will result in a symmetrical breaking of the stop band of the Bragg reflector and hence a dip in the reflectance peak (Pavesi and Mulloni, 1998; Weiss and Fauchet, 2003).

The first microcavity, MC-1, designed with H and L refractive indices of 1.25 and 1.8, respectively, was applied for the resazurin stability studies. The second sample, MC-2, was designed as a sensing platform for LDH. In order to ensure sufficient infiltration of the enzyme in the porous structure, especially in the spacer layer, larger pore sizes were used for the L layer compared to MC-1. As a consequence, the porosity of the L layer was higher than for MC-1 which resulted in a 45% decrease of the refractive index contrast.

The experimental reflectance spectra under normal illumination of MC-1 and MC-2 were compared with the corresponding best-fit simulations obtained by applying the transfer matrix method. Good agreement between the experimentally observed and the simulated cavity modes was observed for both microcavities (see Fig. S1 – Supporting Information). The cavity mode of both MC-1 and MC-2 samples at normal incidence was positioned at 639 nm. In the case of MC-1, the full width at half maximum (FWHM) was ~24 nm, while MC-2 has a larger FWHM of ~32 nm as a consequence of the lower refractive index contrast between the L and H layers. The Q value, *i.e.* the amount of energy stored within the microcavity (Jenie et al., 2014; Ouyang and Fauchet, 2005), was 27 and 20 for MC-1 and MC-2, respectively. Pore sizes were in the range of 39–48 nm for the L layer and 65–100 nm for the H layer. This range of pore size was deemed to be sufficient to allow the infiltration of the enzyme. The microcavity is indeed ~2 μm thick and features the desired $(HL)_3$–HHHH–$(LH)_3$ structure as shown in Fig. S2 (Supporting Information).

3.2. Resazurin immobilisation on pSi samples

The freshly etched samples were chemically modified in order to immobilise resazurin on the surface. As shown in Scheme 1, two different pathways were evaluated. In the first pathway, freshly etched samples underwent thermal hydrosilylation with neat undecylenic acid to introduce the carboxyl groups required to bind resazurin. In the second pathway, we conducted thermal hydrocarbonisation (THC) on the freshly etched surface prior to thermal hydrosilylation, which leads to a passivating hydrocarbon layer on the surface whilst providing reactive sites for the thermal hydrosilylation to occur (Jalkanen et al., 2012a). In both pathways (without and with THC), the carboxyl-terminated samples generated after thermal hydrosilylation underwent acid chloride formation with neat thionyl chloride, followed by substitution of the chlorine moiety with the hydroxyl group of resazurin, forming an ester of the dye on the surface.

The modifications of the samples were followed by FT-IR in reflectance mode. The FT-IR spectra for the two different pathways are shown in Fig. 1. The FT-IR spectrum of the thionyl chloride modified sample was not shown since these samples were highly reactive and needed to be immediately reacted with resazurin.

Spectrum 1 in Fig. 1(a) and (b) exhibits bands at 916 cm^{-1} and 2100 cm^{-1} assigned to the Si–H_2 scissor bending and Si–Hx stretching, respectively, from the hydride species in the freshly etched samples. In the first pathway, thermal hydrosilylation of the freshly etched samples was confirmed by bands observed at 1714, 2890 and 2940 cm^{-1} (Fig. 1(a) – Spectrum 2) corresponding to the νC=O stretching vibrational mode of the carboxylic acid and the νCH_2 stretching vibrational modes of aliphatic C–H bonds, respectively (Boukherroub et al., 2002). Additionally, the disappearance of the silicon hydride band further confirms that Si–Hx was consumed by the undecylenic acid. Further reaction with thionyl chloride and resazurin (Fig. 1(a) – Spectrum 3) shows a distinctive band at 1354 cm^{-1} which was assigned to the νN–O bond of the dye (Das et al., 2013), while bands at 1457 and 1538–1592 cm^{-1} were attributed to the νC–C stretching of the aromatics. The carbonyl peak at 1714 cm^{-1}shifted to 1704 cm^{-1} consistent with ester formation.

In the second pathway, after THC of the freshly etched surface, a strong peak around 1000 cm^{-1} and a new peak at 3010 cm^{-1} (Fig. 1(b) – Spectrum 2) are observed, which are related to the formed hydrocarbon layer (Salonen et al., 2004). Thermal hydrosilylation of the THC modified surface was confirmed by

appearance of the band at 1716 cm^{-1} (Fig. 1(b) – Spectrum 3) attributed to the $\nu C{=}O$ stretching vibrational mode of the carboxylic acid. Bands observed at 1477, 2890 and 2940 cm^{-1} correspond to $-\nu CH_2$ deformation and stretching vibrational modes, respectively (Boukherroub et al., 2002). The spectra of the thermal hydrosilylated samples without and with THC (Fig. 1(a) – Spectrum 2 and Fig. 3(b) – Spectrum 3, respectively) feature similar peaks. This is in agreement with previous work conducted by Jalkanen et al. (2012a), which showed that THC surfaces still provide reactive sites for hydrosilylation with undecylenic acid. Immobilisation of resazurin was again confirmed through the appearance of bands at 1275, 1436, 1475, 1544–1581 and 1750 cm^{-1} (Fig. 1(b) – Spectrum 4) attributed to the νNO bond, the $\nu C{-}C$ stretching of the aromatics and the $\nu C{=}O$ mode of the ester, respectively.

3.3. Stability studies of resazurin on pSi surface

Resazurin is a weakly fluorescing dye which forms the highly fluorescent resorufin upon reduction (O'Brien et al., 2000; Candeias et al., 1998). Resazurin is a good electron acceptor (O'Brien et al., 2000), therefore it is sensitive to the redox status of the environment. Since we previously observed that pSi can reduce resorufin (Low et al., 2006), the stability of the immobilised resazurin on the pSi surface needed to be evaluated.

For the stability study, we performed a simple reaction test using the organic catalyst PMS^+ and coenzyme NADH on resazurin-modified surfaces from both pathways (Candeias et al., 1998). The stability of resazurin on the pSi samples was evaluated by recording the emission spectra of the resazurin-modified MC-1 samples before and after the reaction (Fig. 2) upon excitation at 545 nm.

For samples prepared using the first pathway without THC, the initial spectrum before reduction already showed a broad peak around 585 nm (black dashed curve, Fig. 2(a)). This indicates that the reduction of resazurin into resorufin had already taken place before the addition of PMS^+ and NADH during the 20 min immobilisation of resazurin and caused by the defects in the thermal hydrosilylated pSi. Previous studies have shown that pSi surfaces without proper passivation may act as a reducing agent in which surface oxidation may easily occur on surface defects (Anderson et al., 2003; Low et al., 2006). We investigated further by measuring the fluorescence emission at 585 nm of the resazurin-modified surface in buffer over 90 min (Fig. 2(b)). We observed that the intensity started to increase over the first 30 min of incubation and then reached a plateau, confirming the reduction reaction on the thermal hydrosilylated pSi in the absence of LDH.

To increase the stability of the surface, the samples were treated with THC prior to thermal hydrosilylation. As shown in Fig. 2(a) (red dashed curve), the spectrum before the reaction showed low emission indicating that reduction had not occur before the reduction with NADH and PMS^+. And the time trace in Fig. 2(b) shows that the fluorescence from the surface was stable over the time frame of the experiment (90 min), which is sufficiently long for a biosensor experiment. The fluorescence actually decreased somewhat over time, which we attributed to photobleaching effects. These results corroborate the predicted stability of the THC-modified samples (Jalkanen et al., 2012a, 2012b). We suggest that the relatively higher stability of the THC-thermally hydrosilylated samples over the ones without THC is attributed to the hydrocarbon layer formed on the THC samples that prevents the pSi surface from being oxidised. In addition, THC surfaces have been reported to be more hydrophobic (Jalkanen et al., 2012b; Salonen et al., 2004), therefore making them more stable in aqueous solutions. In both pathways, after catalytic reduction with PMS^+ and NADH, the resazurin-modified MC-1 sample shows narrow emission with maximum at 585 nm (Fig. 2(a)). This was

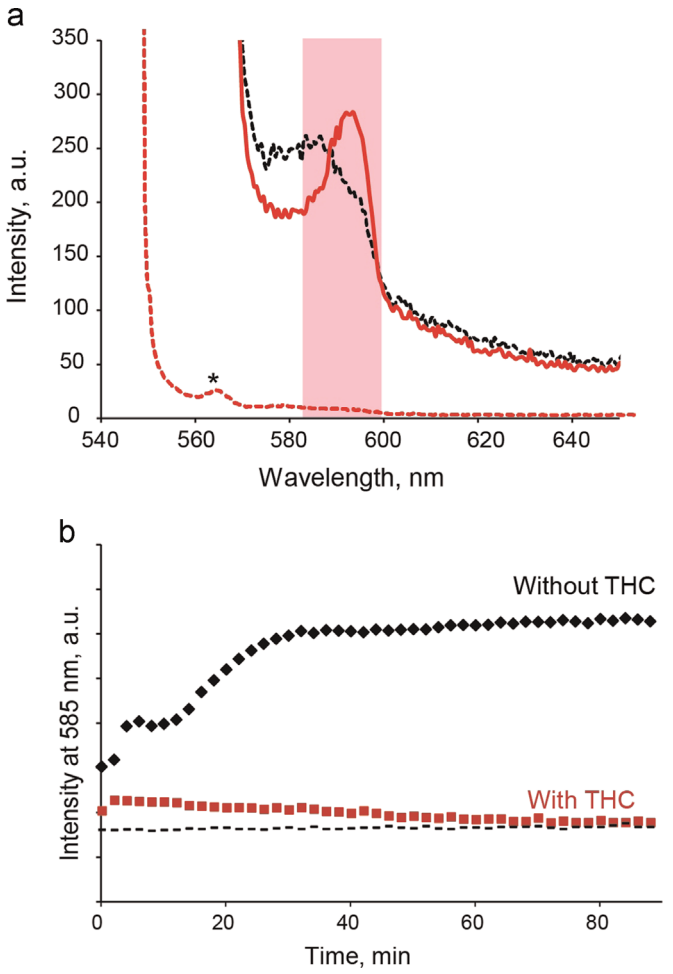

Fig. 2. (a) Emission spectra at 585 nm (pink shaded area, λ_{exc} 545 nm) of the resazurin-modified MC-1 surface before (dashed curves: black – without THC, red – with THC) and after (red solid curve) reduction with NADH and PMS^+. (*The peak at 565 nm corresponds to the interference reflectance peak from MC-1) (b) Changes in emission intensities of the resazurin-modified samples ((♦) without THC, (■) with THC and (–) control MC-1 not modified with resazurin) *vs.* time monitored at 585 nm. (For interpretation of the references to colour in this figure legend, the reader is referred to the web version of this article.)

expected due to the confined light inside the spacer layer and the smaller bandwidth of MC-1 (~24 nm) compared to the bandwidth of resorufin in solution (~46 nm).

3.4. Optical properties of the sensing platform

Due to the high stability provided by thermal hydrocarbonisation, the second pathway was chosen for chemically modifying the pSi samples in preparation for the sensing experiments. Sample MC-2 was used here as the sensing platform due to its larger pores in the L layer compared to MC-1. The L layer in MC-2 has a pore size range of 39–48 nm, which allows infiltration of the LDH enzymes (MW 140 kDa, crystal size of 100.3 Å (Dym et al., 2000)) inside the pores. The evolution of the reflectance spectra of MC-2 at each stage of the surface functionalisation process were measured in air at normal incidence, as shown in Fig. S5 (Supporting Information). The optical response of the microcavity structure was recorded in order to assess changes in the optical quality upon surface modification, as well as to define the position of the cavity mode after each modification step. Initially, a blue-shift of ~2 nm was observed after THC of a freshly etched sample. This shift was due to the decrease of the refractive index caused by the formation of a hydrocarbon layer upon THC (Jalkanen et al.,

2012b). After thermal hydrosilylation, a redshift of ~9 nm was detected, confirming the formation of the undecylenic acid monolayer on the surface. Incubation with resazurin resulted in a redshift of ~4 nm, confirming immobilisation of the molecule. The amount of resazurin immobilised on the surface after incubation with 1 mg/ml resazurin solution was 0.0238 mg/cm^2 (see Supporting Information).

The optical quality of the freshly etched and functionalised MC-2 was preserved with a Q-value maintained at ~20 for each reflectance spectra (Fig. S3). The final position of the resonance wavelength of the resazurin-modified MC-2 was measured at 651 nm at normal incidence. At 45° incidence, the resonance wavelength blueshifts and overlaps with the emission of the resorufin at 585 nm.

3.5. Towards an optical LDH biosensor

The main principle of the detection of LDH is that the enzyme catalyses the interconversion of L-lactate and pyruvate, in the presence of its coenzyme NAD$^+$/NADH. In this study, we worked on the oxidative direction where LDH oxidises the substrate L-lactate into pyruvate while simultaneously reducing NAD$^+$ into NADH. The reason for this is because the LDH enzyme used in this study originates from heart tissue (H4-LDH). The H subunit is inhibited by pyruvate, hence it shows higher affinity towards the production of pyruvate (Bittar et al., 1996). The enzymatic reaction was coupled to the resazurin reduction. The increase of emission at 585 nm corresponding to formation of resorufin is proportional to the amount of LDH present. This detection principle was translated onto the pSi surface. Scheme 2 illustrates the detection mechanism on the MC-2 sample.

The resazurin-modified MC-2 was exposed to a solution of PMS$^+$ (300 μM), β-NAD$^+$ (1 mM), L-lactate (35 mM) and LDH for 10 min at 37 °C. The concentration of LDH used in this experiment was 16.26 U/ml. The spectrum in Fig. 3(a) shows the emission of resorufin with a maximum at 590 nm and a narrow FWHM of ~12 nm. This emission bandwidth is 26% narrower compared to the broad emission spectrum of resorufin in solution (FWHM ~46 nm, Fig. S6 – Supporting Information). The narrowing of the emission spectrum is again attributed to the light confinement inside the spacer layer of the microcavity structure. However, the emission bandwidth of resorufin in MC-2 is 50% broader than that of MC-1 (FWHM ~8 nm), which is expected since the refractive index contrast of MC-2 is lower than MC-1. Fig. 3(a) also illustrates the alignment of the emission spectrum and the simulated reflectance spectrum of the modified surface at 45°. The reflectance spectrum was generated by performing the best fit of the experimental reflectance spectrum of the resazurin-modified MC-2 at normal incidence, and using the calculated effective refractive indices of the layers by means of the transfer matrix method.

To demonstrate the fluorescence enhancement using the pSiMC due to the confinement of light in the spacer layer of the resonant structure of MC-2, we compared the emission intensity after incubation with LDH with other pSi architectures, i.e single layer and a detuned microcavity (detuned-MC). The single layer consists of one H layer with 84% porosity, while the detuned MC has the same structure as MC-2 but different thickness of the H and L layers (Table S1 – Supporting Information). The detuned-MC is not aligned with the maximum emission of the resorufin (585 nm). Both structures have the same total thickness to MC-2 of 2 μm. Fig. 3(b) shows that the emission intensity using MC-2 was 10- and 5-fold higher than using single layer and detuned MC, respectively. This is in agreement with previous studies showing that a microcavity featuring a good spectral alignment with the maximum emission of the emitting molecule enhances the emission intensity of the immobilised fluorophore (DeLouise and Ouyang, 2009; Palestino et al., 2009). When we partially masked the surface of the resazurin-modified MC-2 during 10 min exposure to LDH (Fig. 3(c)), only the part of the surface exposed to LDH showed surface fluorescence emission in a confocal microscopy image upon excitation at 561 nm (Fig. 3(d)).

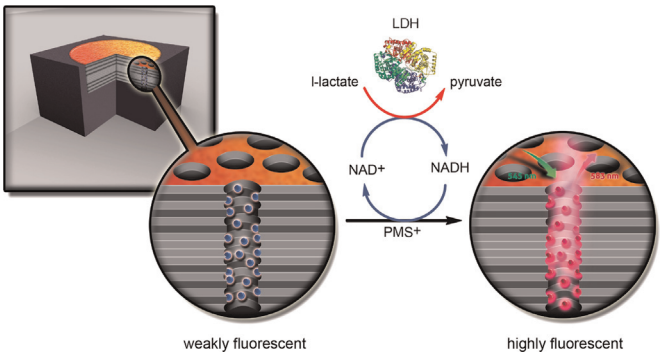

Scheme 2. LDH detection scheme on resazurin-modified pSiMC surface.

Having successfully demonstrated the detection of LDH *via* fluorescence enhancement on the MC-2 sample, we further investigated the analytical performance of the biosensor. The amount of LDH in normal human blood serum ranges from 0.1 to 0.3 U/ml (James et al., 2000; Kato et al., 2006) and an increase to over 1 U/ml indicates tissue or cellular damage (Ren et al., 2010; Yang et al., 2011). However, studies have shown that LDH levels lower than 1 U/ml are already indicative of pathological conditions. Kato et al. (2006) reported that LDH levels above 0.5 U/ml relates to haemolysis-associated nitric oxide resistance which is one of the endothelial dysfunction in patients with sickle cell disease, while in breast and ovarian cancers the LDH levels are over 0.3 U/ml (Koukourakis et al., 2009). LDH concentrations in wound fluid of 3–5 U/ml have been reported (James et al., 2000).

MC-2 samples were exposed to different concentrations of LDH ranging from 0.02 to 16.26 U/ml in Tris-buffer. Assays were performed in triplicate. Fig. 4 shows the correlation between the LDH concentration in buffer and the fluorescence intensity of the modified surface at 585 nm. At low concentrations, the emission does not differ from the one of the blank control. A linear relationship between the emission intensity and the concentration of LDH was observed over the range of 0.16–6.5 U/ml ($y=156.09x+251.16$ ($R^2=0.9844$)). Therefore, our platform is able to detect the activity of LDH in normal as well as in damaged tissues. The working concentration range of the biosensor is wider than those based on QDs (Yang et al., 2011) and QDs incorporated nanofibers (He et al., 2012), 0.25–6 U/ml and 0.2–2.4 U/ml, respectively. The limit of detection (LOD) was 0.08 U/ml, calculated using the equation of y_b+3Std_b, where y_b is the average of the emission intensity measured for the blank control and Std_b is the associated standard deviation (Krismastuti et al., 2014). The LOD was comparable to the QDs-based LDH biosensor of 0.075 U/ml (Ren et al., 2010). LDH biosensor based on the amperometric method have been reported to have slightly lower LOD (0.05 U/ml) (Hong et al., 2002). However, this particular biosensor only shows a linear response up to 0.5 U/ml, less than the required level to detect cellular or tissue damage.

We further examined the selectivity of the biosensor by exposing it to another NAD-dependant dehydrogenase enzyme, L-glutamic dehydrogenase (GDH), in the same buffer. The results showed that the biosensor is not responding to the presence of GDH (Fig. S7 – Supporting Information).

Finally, the developed LDH sensing platform was more cost-effective and faster in terms of the reagents consumed and the incubation time, respectively, compared to the standard LDH protocols, such as the ones developed by OPS Diagnostics (LLC,

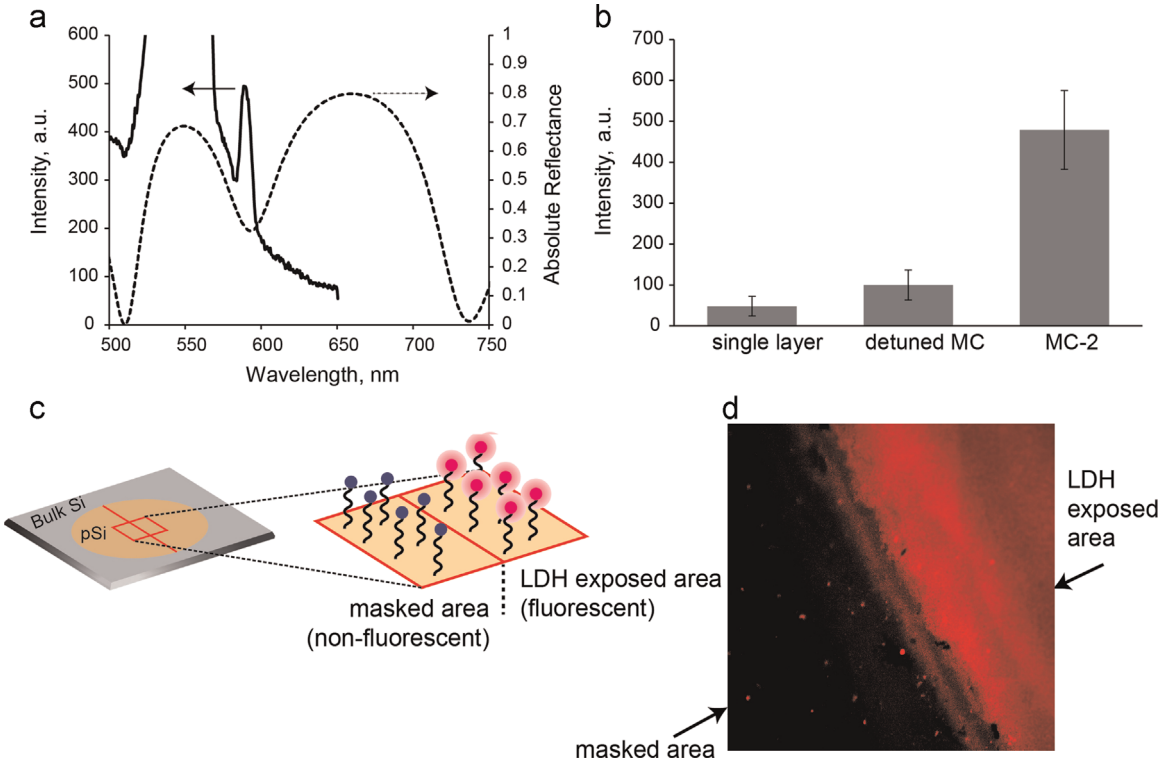

Fig. 3. (a) The emission spectrum (solid line) of resazurin-modified MC-2 after incubation with LDH (16.26 U/ml) in Tris-Buffer (pH 8.6) at an excitation wavelength of 545 nm. The emission spectrum was overlayed with the simulated reflectance spectrum at 45° (dashed line) of resazurin-modified MC-2. (b) Comparison of emission intensities of MC-2 with other different pSi surface structures (*i.e.* single layer and detuned MC) of the same thickness after incubation with LDH (16.26 U/ml) in Tris-Buffer (pH 8.6) at an excitation wavelength of 545 nm. The error bars were obtained after conducting three separate experiments. (c) Schematic of the resazurin-modified MC-2 with half of the surface masked upon LDH incubation. (d) Confocal microscopy image of the partially masked resazurin-modified MC-2 (excitation 561 nm, emission range 576–701 nm).

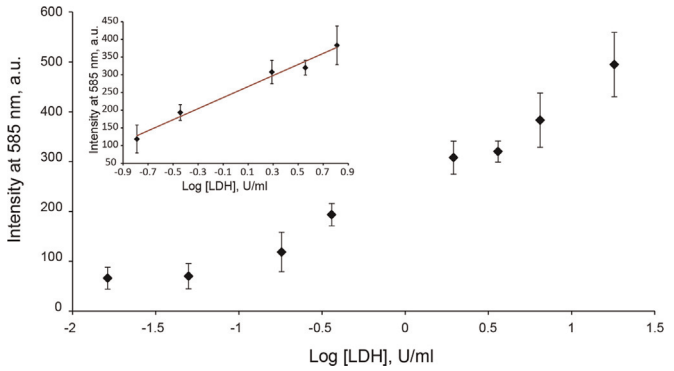

Fig. 4. Response of the emission intensity of resazurin-modified MC-2 at 585 nm *vs.* LDH concentration after 10 min incubation. The inset shows the linear relationship over the concentration range from 0.16 to 6.5 U/ml.

Lebanon, NJ, USA). Using the same coenzyme and substrate, this commercial assay determines LDH levels by measuring the absorbance of formazan at 490 nm (Cohen et al., 2013). As earlier mentioned, the reduction of INT was coupled to the interconversion of L-lactate/pyruvate and NAD^+/NADH in the presence of LDH. Overall, our sensing platform reduces the consumption of the reagents involved (*i.e.* NAD^+, L-lactate and PMS^+) by over 30% compared to the standard assay for LDH in solution. Our system shows a strong response after 10 min of incubation of the resazurin-modified MC-2 samples with LDH. In contrast, the standard assay takes 30 min to perform.

4. Conclusions

We have demonstrated the detection of LDH on a resazurin-modified pSiMC by exploiting fluorescence enhancement effects inside pSi microcavities upon enzyme-catalysed formation of resorufin. The covalent immobilisation of resazurin on the surface was achieved through a four-step surface chemistry consisting of thermal hydrocarbonisation with acetylene, thermal hydrosilylation with undecylenic acid, acid chloride formation with thionyl chloride and finally acylation of resazurin. FTIR and the optical shift of the resonance wavelength of the microcavity were used to confirm each modification step. Thermal hydrocarbonisation followed by thermal hydrosilylation conveyed excellent stability to the resazurin-modified surface, ensuring that resazurin is not reduced prior to detection. The fluorescence intensity measured upon LDH detection on pSi microcavities was 10- and 5-fold higher than that on single layer and detuned microcavity, respectively. This signal enhancement led to an excellent limit of detection of 0.08 U/ml with a linear response between 0.16 and 6.5 U/ml. The biosensor demonstrated here is expected to find applications in point-of-care diagnostics of chronic wounds, cancer and other pathologies where isoforms of LDH serve as biomarkers.

Acknowledgements

The authors would like to thank Dr. Steven J.P. McInnes for fruitful discussions, Marc Cirera for the graphical image of the LDH detection in Scheme 2 and Dr. Roey Elnathan for performing the confocal microscope imaging. This research was conducted and funded by the Australian Research Council Centre of Excellence in Convergent Bio-Nano Science and Technology (Project number CE140100036). SNAJ would like to thank the Australian Government for the Australia Award Scholarship and acknowledge funding from the Wound Management Innovation CRC (Australia).

Appendix A. Supporting material

Supporting data associated with this article can be found in the online version at http://dx.doi.org/10.1016/j.bios.2015.07.025.

References

Anderson, S.H.C., Elliott, H., Wallis, D.J., Canham, L.T., Powell, J.J., 2003. Phys. Status Solidi A 197 (2), 331–335.
Bisswanger, H., 2014. Perspect. Sci. 1 (1–6), 41–55.
Bittar, P.G., Charnay, Y., Pellerin, L., Bouras, C., Magistretti, P.J., 1996. J. Cereb. Blood Flow Metab. 16 (6), 1079–1089.
Bosch, M., Sánchez, A., Rojas, F., Ojeda, C., 2007. Sensors 7 (6), 797–859.
Boukherroub, R., Wojtyk, J.T.C., Wayner, D.D.M., Lockwood, D.J., 2002. J. Electrochem. Soc. 149 (2), H59–H63.
Chen, Y., Zhang, H., Xu, A., Li, N., Liu, J., Liu, C., Lv, D., Wu, S., Huang, L., Yang, S., He, D., Xiao, X., 2006. Lung Cancer 54 (1), 95–102.
Cohen, S.S., Min, M., Cummings, E.E., Chen, X., Sadowska, G.B., Sharma, S., Stonestreet, B.S., 2013. Neuroimmunomodulation 20 (5) 10.1159/000350470.
Candeias, L.P., MacFarlane, D.P.S., McWhinnie, S.L.W., Maidwell, N.L., Roeschlaub, C. A., Sammes, P.G., Whittlesey, R., 1998. J. Chem. Soc. Perkin Trans. 2 (11), 2333–2334.
Das, R.S., Singh, B., Banerjee, R., Mukhopadhyay, S., 2013. Dalton Trans. 42 (11), 4068–4080.
Decker, T., Lohmann-Matthes, M.-L., 1988. J. Immunol. Methods 115 (1), 61–69.
DeLouise, L.A., Kou, P.M., Miller, B.L., 2005. Anal. Chem. 77 (10), 3222–3230.
DeLouise, L.A., Ouyang, H., 2009. Phys. Status Solidi C 6 (7), 1729–1735.
Drent, M., Cobben, N., Henderson, R., Wouters, E., van Dieijen-Visser, M., 1996. Eur. Respir. J. 9 (8), 1736–1742.
Dym, O., Pratt, E.A., Ho, C., Eisenberg, D., 2000. Proc. Natl. Acad. Sci. 97 (17), 9413–9418.
He, X., Tan, L., Wu, X., Yan, C., Chen, D., Meng, X., Tang, F., 2012. J. Mater. Chem. 22 (35), 18471–18478.
Ho, J., de Moura, M.B., Lin, Y., Vincent, G., Thome, S., Duncan, L.M., Hui-Min, L., Kirkwood, J.M., Becker, D., Van Houten, B., Moschos, S.J., 2012. Mol. Cancer 11 (1), 76–88.
Hong, M.-Y., Chang, J.-Y., Yoon, H.C., Kim, H.-S., 2002. Biosens. Bioelectron. 17 (1–2), 13–18.
Hou, J.-M., Greystoke, A., Lancashire, L., Cummings, J., Ward, T., Board, R., Amir, E., Hughes, S., Krebs, M., Hughes, A., Ranson, M., Lorigan, P., Dive, C., Blackhall, F.H., 2009. Am. J. Pathol. 175 (2), 808–816.
Ispas, C.R., Crivat, G., Andreescu, S., 2012. Anal. Lett. 45 (2–3), 168–186.
Jalkanen, T., Mäkilä, E., Sakka, T., Salonen, J., Ogata, Y., 2012a. Nanosc. Res. Lett. 7 (1), 1–6.
Jalkanen, T., Mäkilä, E., Suzuki, Y.I., Urata, T., Fukami, K., Sakka, T., Salonen, J., Ogata, Y.H., 2012b. Adv. Funct. Mater. 22 (18), 3890–3898.
James, T.J., Hughes, M.A., Cherry, G.W., Taylor, R.P., 2000. Wound Repair Regen. 8 (4), 264–269.
Jane, A., Dronov, R., Hodges, A., Voelcker, N.H., 2009. Trends Biotechnol. 27 (4), 230–239.
Janshoff, A., Dancil, K.-P.S., Steinem, C., Greiner, D.P., Lin, V.S.Y., Gurtner, C., Motesharei, K., Sailor, M.J., Ghadiri, M.R., 1998. J. Am. Chem. Soc. 120 (46), 12108–12116.
Jenie, S.N.A., Pace, S., Sciacca, B., Brooks, R.D., Plush, S.E., Voelcker, N.H., 2014. ACS Appl. Mater. Interfaces 6 (15), 12012–12021.
Kastritis, E., Kyrtsonis, M.-C., Hadjiharissi, E., Symeonidis, A., Michalis, E., Repoussis, P., Tsatalas, C., Michael, M., Sioni, A., Kartasis, Z., Stefanoudaki, E., Voulgarelis, M., Delimpasi, S., Gavriatopoulou, M., Koulieris, E., Gika, D., Zomas, A., Roussou, P., Anagnostopoulos, N., Economopoulos, T., Terpos, E., Zervas, K., Dimopoulos, M.A., 2010. Leuk. Res. 34 (10), 1340–1343.
Kato, G.J., McGowan, V., Machado, R.F., Little, J.A., Taylor, J., Morris, C.R., Nichols, J.S., Wang, X., Poljakovic, M., Morris, S.M., Gladwin, M.T., 2006. Blood 107 (6), 2279–2285.
Koenderink, A.F., 2010. Opt. Lett. 35 (24), 4208–4210.
Koukourakis, M.I., Kontomanolis, E., Giatromanolaki, A., Sivridis, E., Liberis, V., 2009. Gynecol. Obstet. Investig. 67 (3), 162–168.
Krismastuti, F.S.H., Pace, S., Melville, E., Cowin, A., Dargaville, T.R., Voelcker, N.H., 2013. Aust. J. Chem. 66 (11), 1428–1434.
Krismastuti, F.S.H., Pace, S., Voelcker, N.H., 2014. Adv. Funct. Mater. 24 (23), 3639–3650.
Larsen, T., 2005. J. Dairy Res. 72 (02), 209–216.
Lin, V.S.-Y., Motesharei, K., Dancil, K.-P.S., Sailor, M.J., Ghadiri, M.R., 1997. Science 278 (5339), 840–843.
Low, S.P., Williams, K.A., Canham, L.T., Voelcker, N.H., 2006. Biomaterials 27 (26), 4538–4546.
Martin, M., Palestino, G., Cloitre, T., Agarwal, V., Zimányi, L., Gergely, C., 2009. Three-Dimensional Spatial Resolution of the Nonlinear Photoemission from Biofunctionalized Porous Silicon Microcavity. AIP.
Moran, J.H., Schnellmann, R.G., 1996. J. Pharmacol. Toxicol. Methods 36 (1), 41–44.
O'Brien, J., Wilson, I., Orton, T., Pognan, F., 2000. Eur. J. Biochem./FEBS 267 (17), 5421–5426.
Ouyang, H., Fauchet, P.M., 2005. Biosensing using porous silicon photonic bandgap structures. In: Proceeding SPIE 6005, Photonic Crystals and Photonic Crystal Fibers for Sensing Applications, pp. 600508–600515.
Pace, S., Vasani, R.B., Cunin, F., Voelcker, N.H., 2013. New J. Chem. 37 (1), 228–235.
Palestino, G., Agarwal, V., Aulombard, R., Pérez, Ea, Gergely, C., 2008. Langmuir 24 (23), 13765–13771.
Palestino, G., Martin, M., Agarwal, V., Legros, R., Cloitre, T., Zimányi, L., Gergely, C., 2009. Phys. Status Solidi C 6 (7), 1624–1628.
Pavesi, L., Mulloni, V., 1998. J. Lumin. 80 (1–4), 43–52.
Poitras, C.B., Lipson, M., Du, H., Hahn, M.A., Krauss, T.D., 2003. Appl. Phys. Lett. 82 (23), 4032–4034.
Purcell, E.M., 1946. Phys. Rev. 69 (11–12), 681.
Qiao, H., Guan, B., Bocking, T., Gal, M., Gooding, J.J., Reece, P.J., 2010. Appl. Phys. Lett. 96 (16), 161106.
Ren, X., Yang, L., Tang, F., Yan, C., Ren, J., 2010. Biosens. Bioelectron. 26 (1), 271–274.
Sailor, M.J., Wu, E.C., 2009. Adv. Funct. Mater. 19 (20), 3195–3208.
Salonen, J., Björkqvist, M., Laine, E., Niinistö, L., 2004. Appl. Surf. Sci. 225 (1–4), 389–394.
Sciacca, B., Frascella, F., Venturello, A., Rivolo, P., Descrovi, E., Giorgis, F., Geobaldo, F., 2009. Sens. Actuators B 137 (2), 467–470.
Setzu, S., Ferrand, P., Romestain, R., 2000. Mater. Sci. Eng. B 69–70 (0), 34–42.
Wang, N., Huang, D., Zhang, J., Cheng, J., Yu, T., Zhang, H., Bi, S., 2008. J. Phys. Chem. C 112 (46), 18034–18038.
Weiss, S.M., Fauchet, P.M., 2003. Phys. Status Solidi A 197 (2), 556–560.
Yang, L., Ren, X., Meng, X., Li, H., Tang, F., 2011. Biosens. Bioelectron. 26 (8), 3488–3493.
Zhao, Y., Zhao, X., Gu, Z., 2010. Adv. Funct. Mater. 20 (18), 2970–2988.
Zhu, A., Romero, R., Petty, H.R., 2010. Anal. Biochem. 396 (1), 146–151.
Zhuang, G.-S., Liu, J., Jia, C.-P., Jin, Q.-H., Zhao, J.-L., Wang, H.-M., 2007. J. Sep. Sci. 30 (9), 1350–1356.